

Operations and Performance of the CMS DT and RPC muon systems

G. Pugliese

INFN & Politecnico of Bari

On behalf of the CMS Collaboration

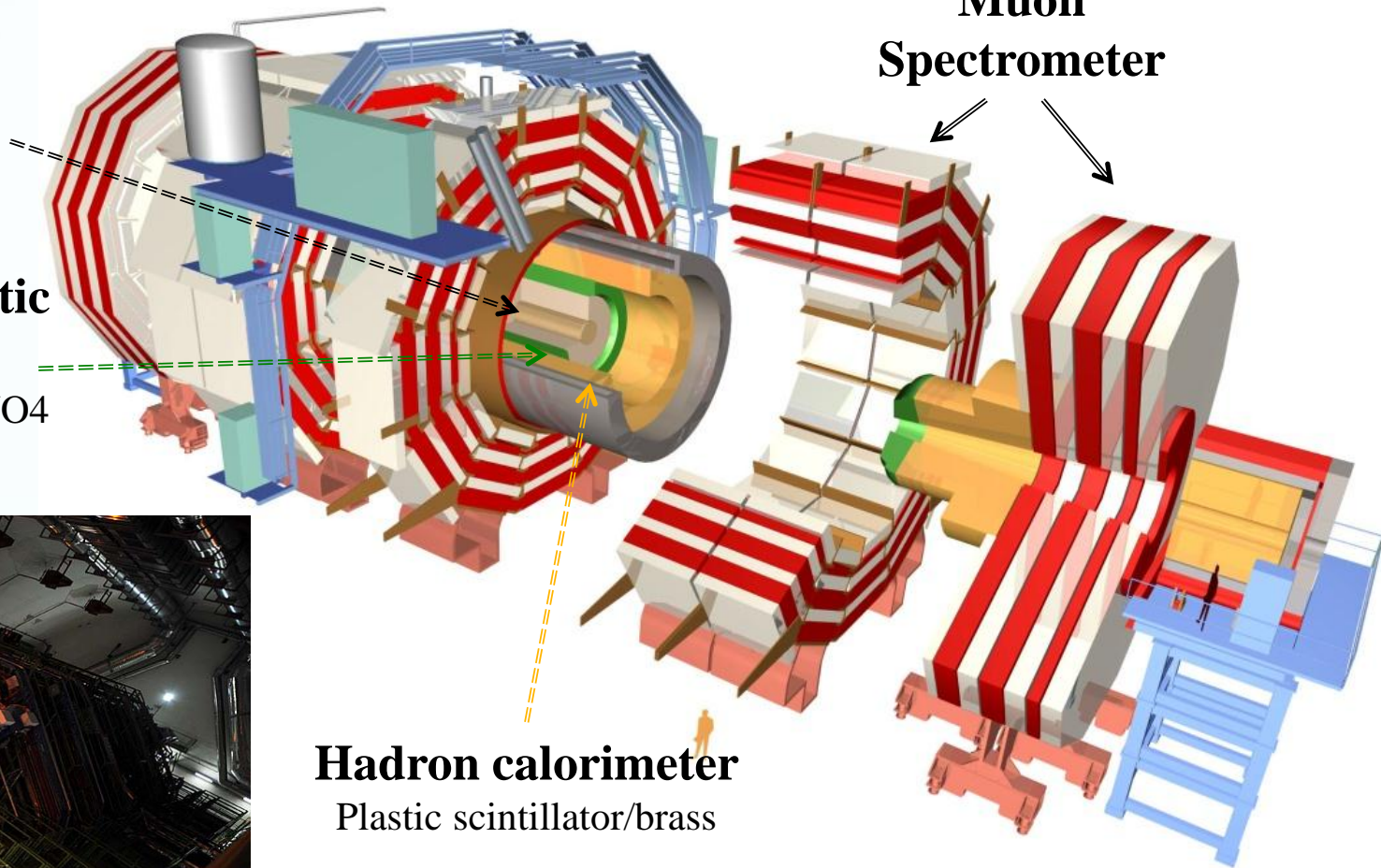
The CMS detector



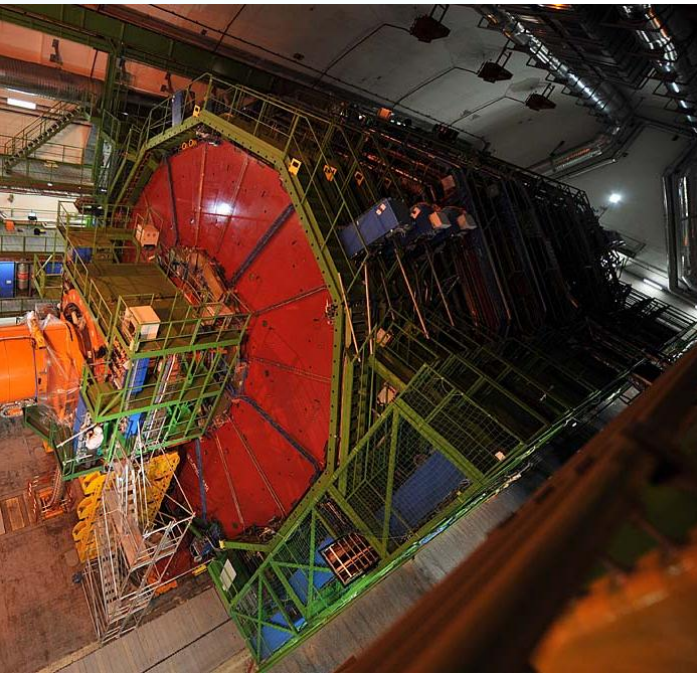
G. Pugliese

**Silicon pixel &
strip tracker**

**Electromagnetic
calorimeter**
(Scintillating PbWO₄
crystals)



Hadron calorimeter
Plastic scintillator/brass



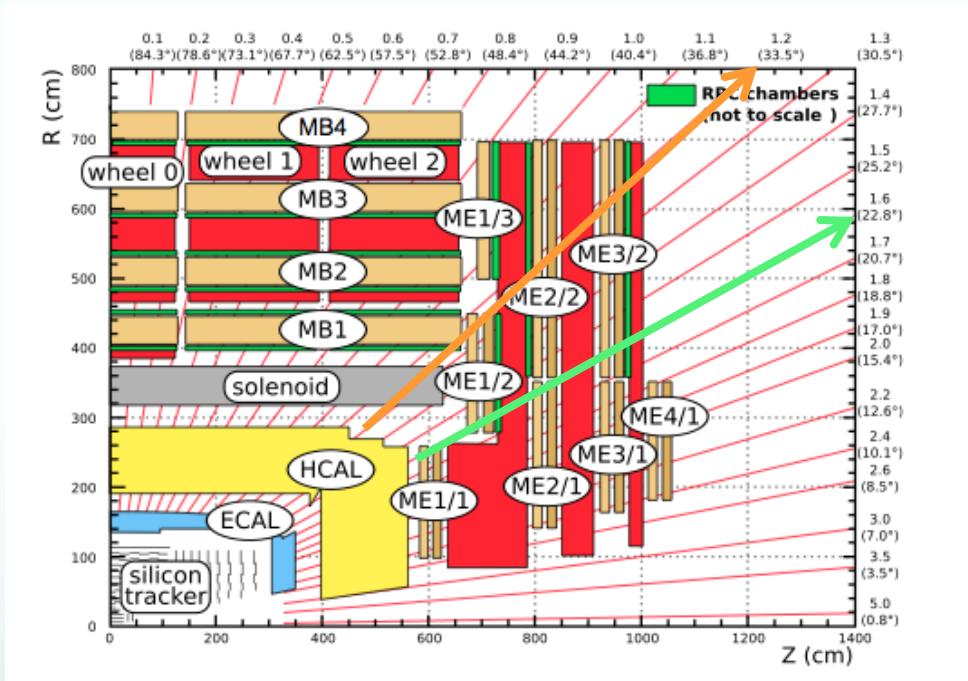
Weight: 12000 t
Length: 21.6 m
Diameter: 15 m
Magnetic field: 3.8 T

The muon spectrometer

G. Pugliese

ICHEP 2012

Robust, efficient and redundant muon system



Planar endcap region:

- **4 planar stations** interleaved with the iron return yoke plates (the 4th will be installed in 2013-14).
- **Cathode Strips Chambers and Resistive Plate Chambers**

Requirement of μ system:

- identification of muons
- measurement of their transverse momentum
- bunch crossing (BX) assignment

Cylindrical barrel region:

- **4 coaxial stations** interleaved with the iron return yoke plates. The stations are grouped into **5 wheels** around the beam line
- **Drift Tube and Resistive Plate Chambers**

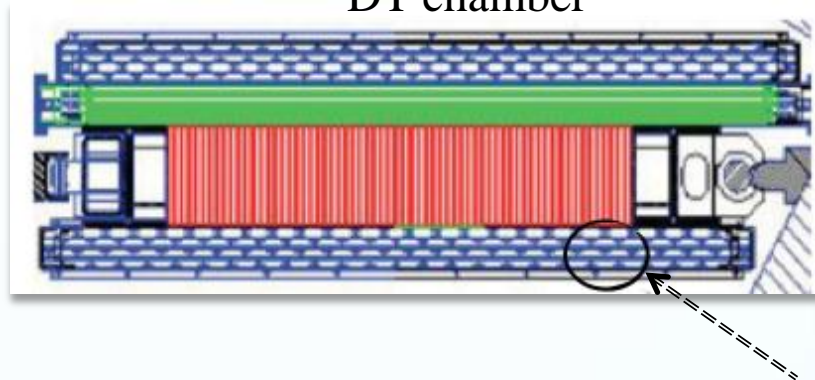
Drift Tube Chambers

G. Pugliese

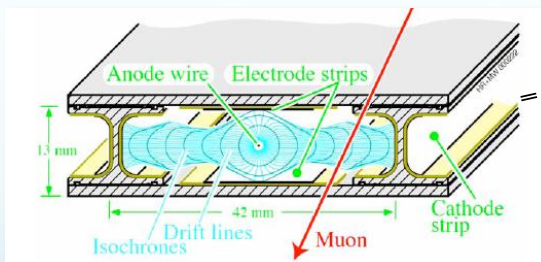
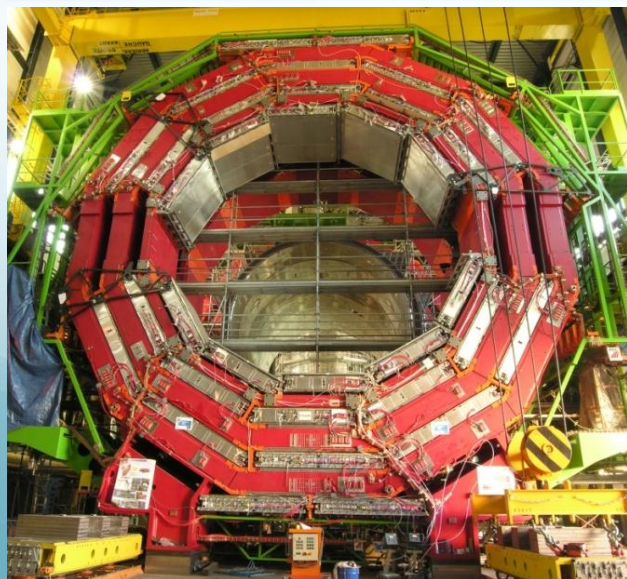
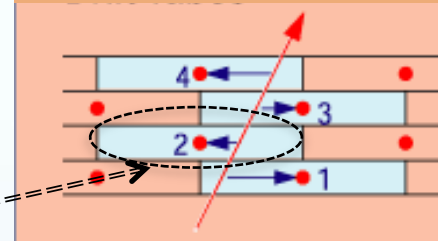
ICHEP 2012

- covers $0 < |\eta| < 1.2$
- 250 **chambers**
- **3 Super Layer/chamber:** 2 SL to measure the $r - \phi$ coordinates and 1 SL the $r - z$ (except for MB4)
- **4 layers/super layer**
- **42 mm x 13 mm cells** for a total of **172000**
- **Gas mixture:** Ar + CO₂ (85 % -15%)

DT chamber



DT Super Layer

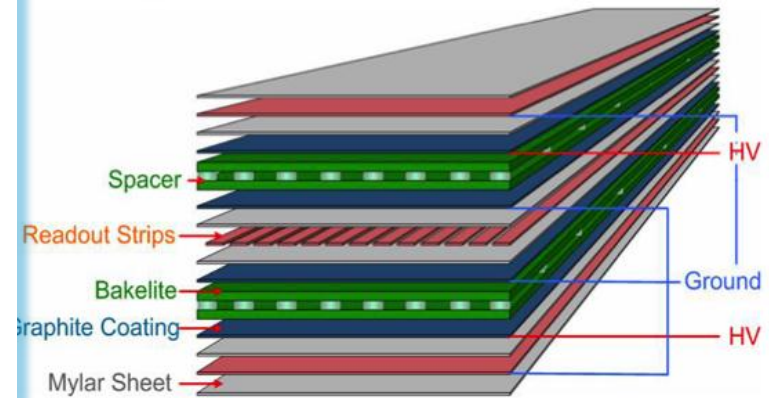


Spatial resolution per wire $\approx 250 \mu\text{m}$
Maximum drift time $\sim 400 \text{ ns}$
Almost linear space-time relationship $\sim 55 \mu\text{m/ns}$

Resistive Plate Chambers

- covers $0 < |\eta| < 1.6$
- **912 chambers** (480 in barrel and 432 in endcap)
- **Double gaps gas chamber:** 2 mm gas width
- 110000 **electronic channels** and 3500 m² of active area
- **Bakelite** bulk resistivity: $\rho = 2-5 \times 10^{10} \Omega\text{cm}$
- **Strip width:** $2 \div 4$ cm.
- **Gas mixture:** $\text{C}_2\text{H}_2\text{F}_4 + \text{isoC}_4\text{H}_{10} + \text{SF}_6$ (40% of H)

95.2%	4.5%	0.3%
-------	------	------
- Operated in **avalanche mode**



Spatial resolution ≈ 1 cm
(depending on strip width)

Time resolution ≈ 2 ns

CMS trigger system

G. Pugliese

Two level trigger system filters out “interesting” events:

Level 1 trigger (made by custom electronic):

40 MHz \rightarrow 100 kHz

latency < 3.2 μ s

High Level trigger (made by a processor farm):

300 Hz

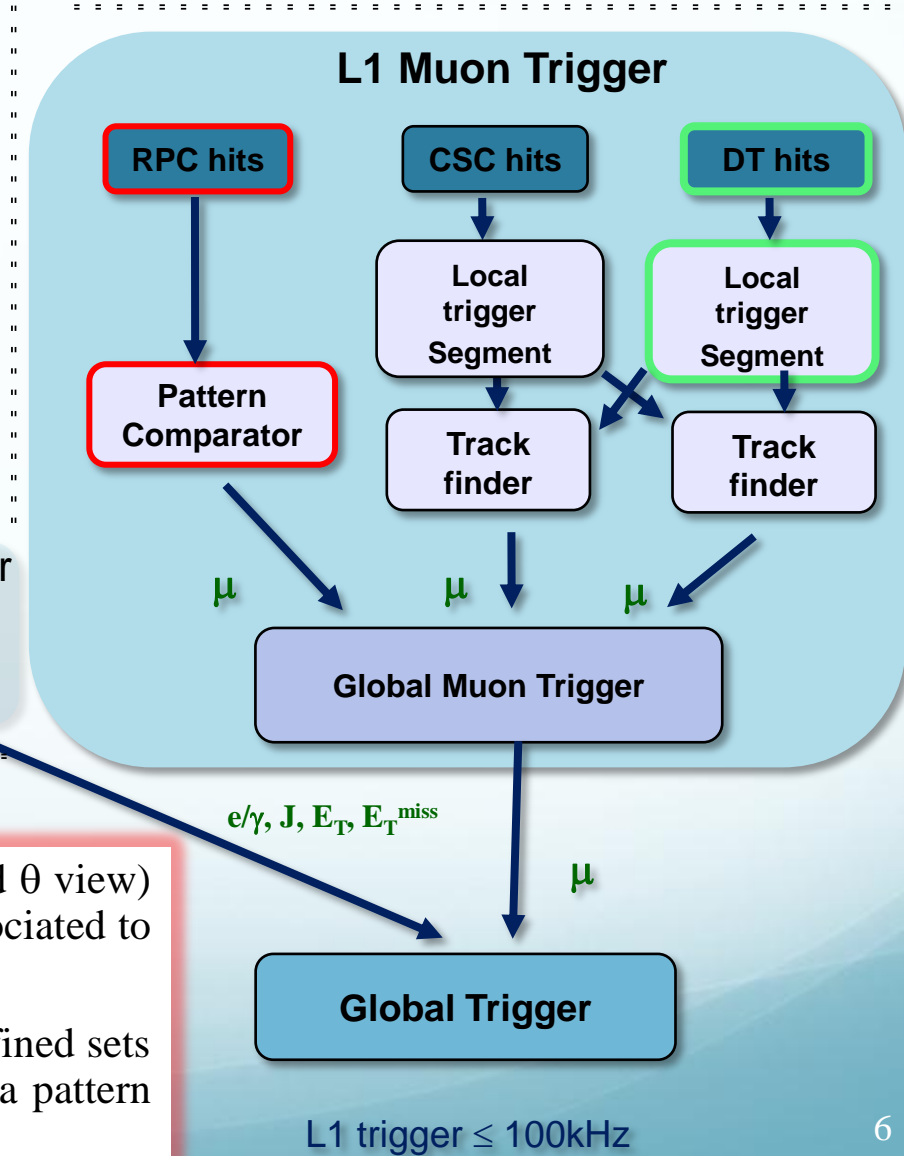
decision made in 1s

L1 Calorimeter Trigger

Global Calorimeter Trigger

DT local trigger: provide **trigger segments** (in ϕ and θ view) for each chamber. Each trigger segment has to be associated to the BX at which the μ candidate was produced.

RPC trigger: the **RPC hits** are compared with predefined sets of patterns. A μ candidate is produced if the hits fit a pattern and are in the same BX.



CMS in operation

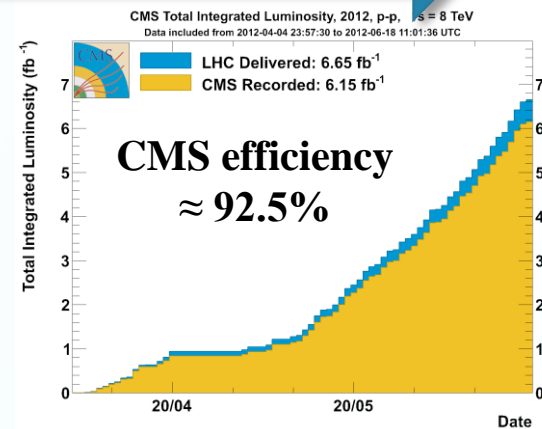
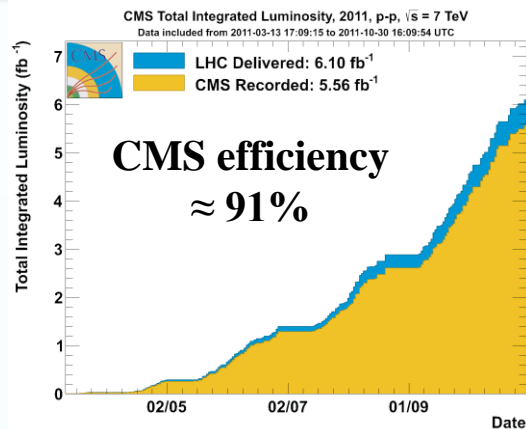
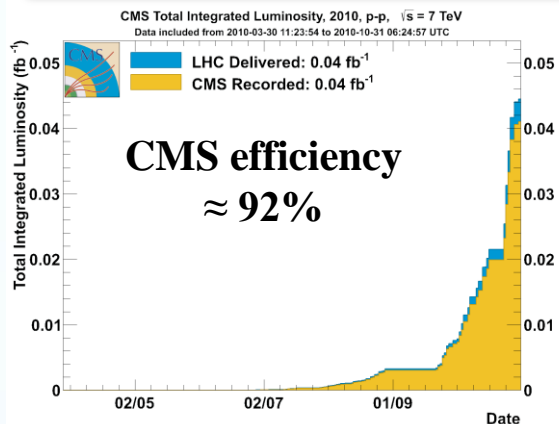
G. Pugliese

ICHEP 2012

2010

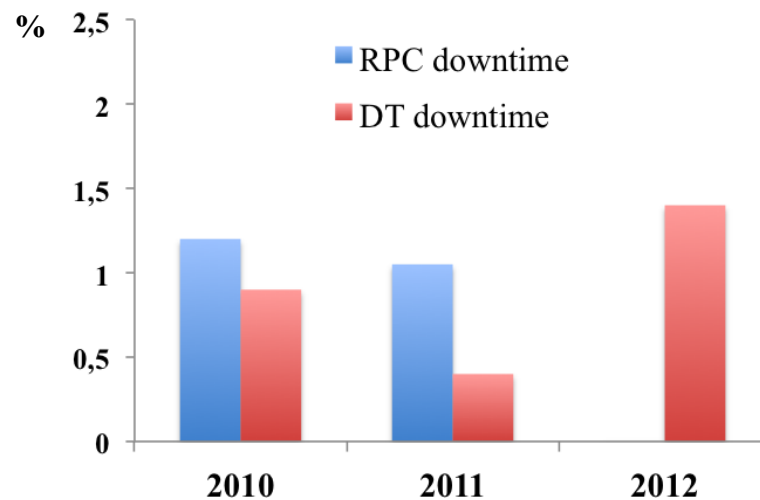
2011

2012



Very high **CMS efficiency** in 2010 and 2011. Even better in 2012.

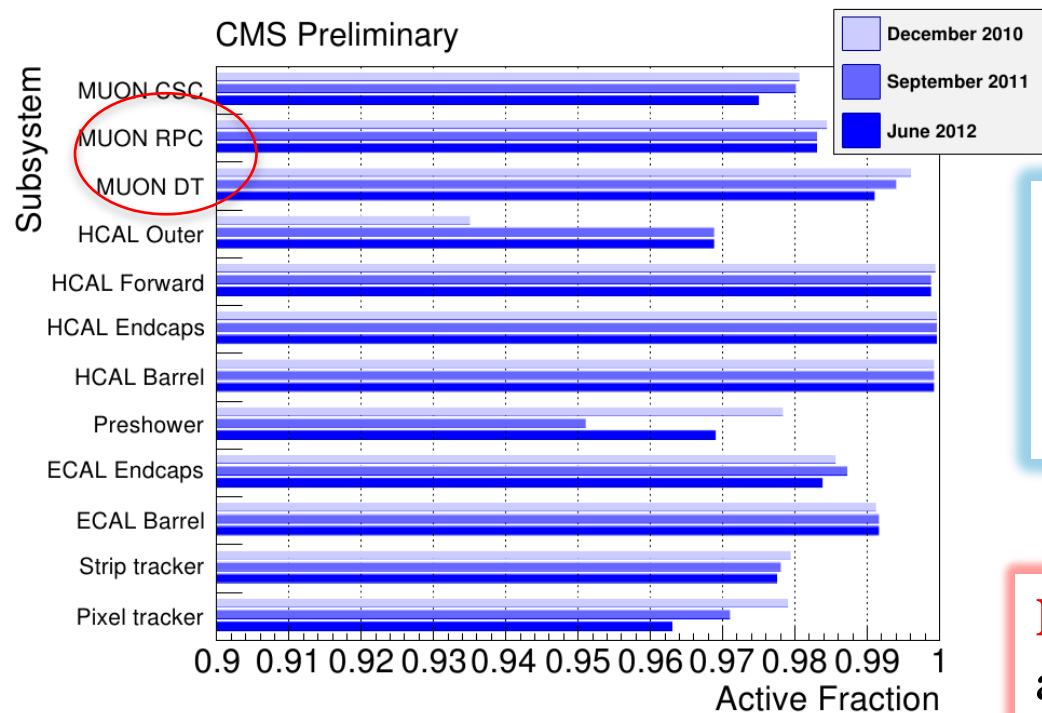
- Very **low contribution of DT and RPC systems** to the **CMS downtime**: less than **1.5 %**.



CMS active channels

G. Pugliese

ICHEP 2012



Fraction of active channels:

- larger then **98%** for RPC. **Stable in time.**
- above **99 %** for DT.

Key of success: clear procedures for a prompt intervention during all beam-off and Technical Access time

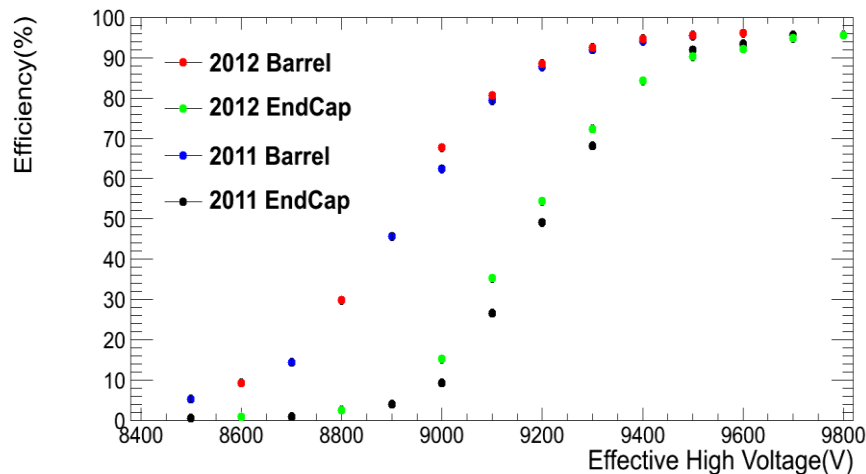
RPC and DT inactive channels are mainly caused by failure of the electronics located near or inside the chambers. Not accessibly since 2009. They will be recovered during long shutdown 2013 -14.

RPC working point calibration

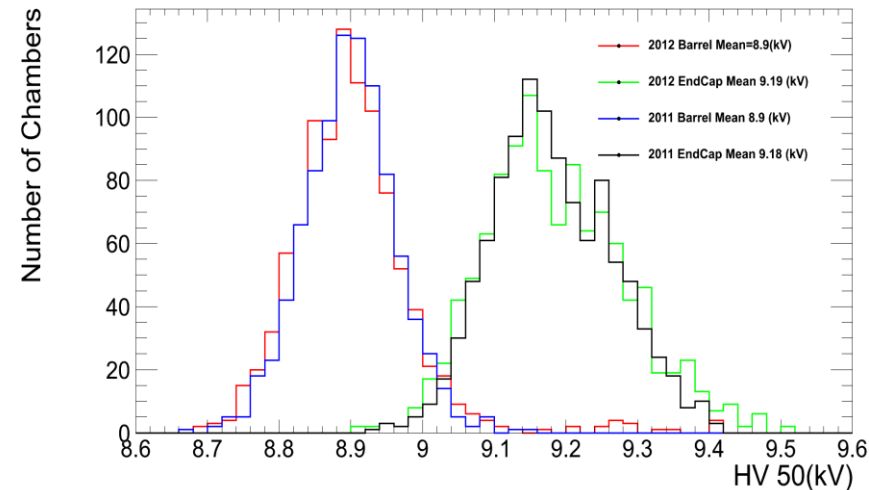
G. Pugliese

ICHEP 2012

At the beginning of 2011 and 2012, an **HV scan** was done in order to study the chambers' Working Point and to monitor in time the performance. The luminosity lost because of the RPC calibration was very low 3.3 pb^{-1} and 6.2 pb^{-1} , in 2011 and 2012.



HV distribution for all RPCs as measured at the 50 % of the efficiency



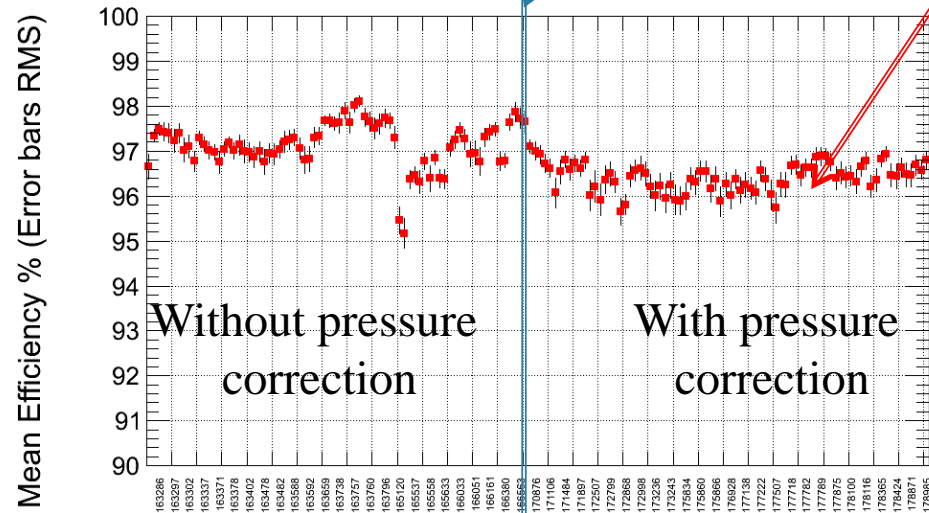
Average efficiency vs HV for all RPCs.

The different WP for Barrel and Endcap chambers depends on different construction techniques used.

RPC performance stability

From **July 2011 on**, the WP is automatically corrected taking into account atmospheric pressure variations. The system is now running more stable.

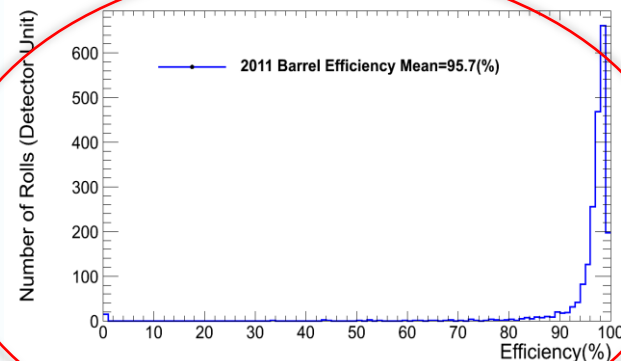
CMS 2011 Preliminary



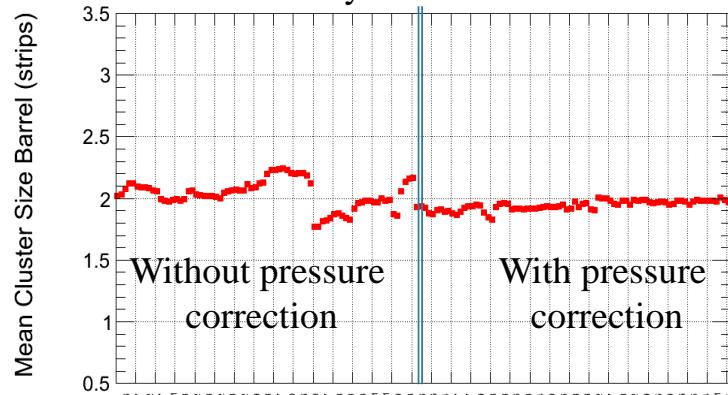
April 2011

October 2011

Barrel average efficiency history



CMS 2011 Preliminary



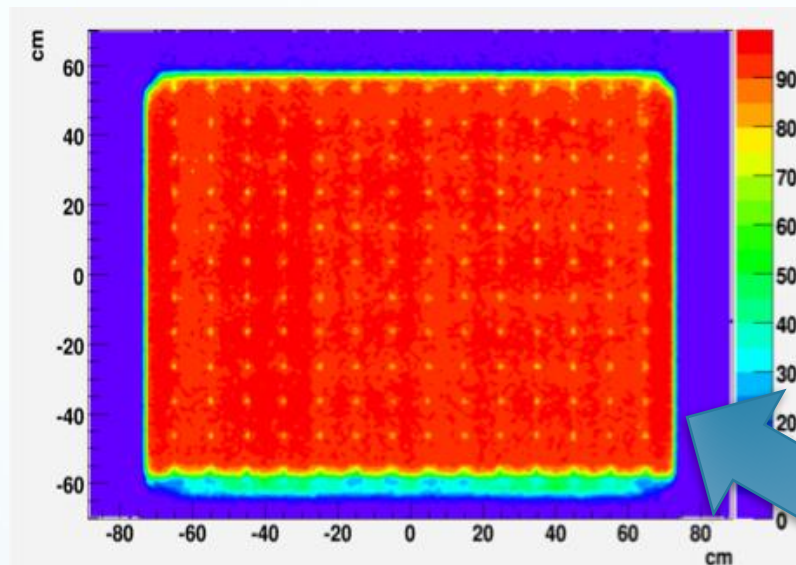
April 2011

October 2011

Barrel cluster size history

RPC efficiency

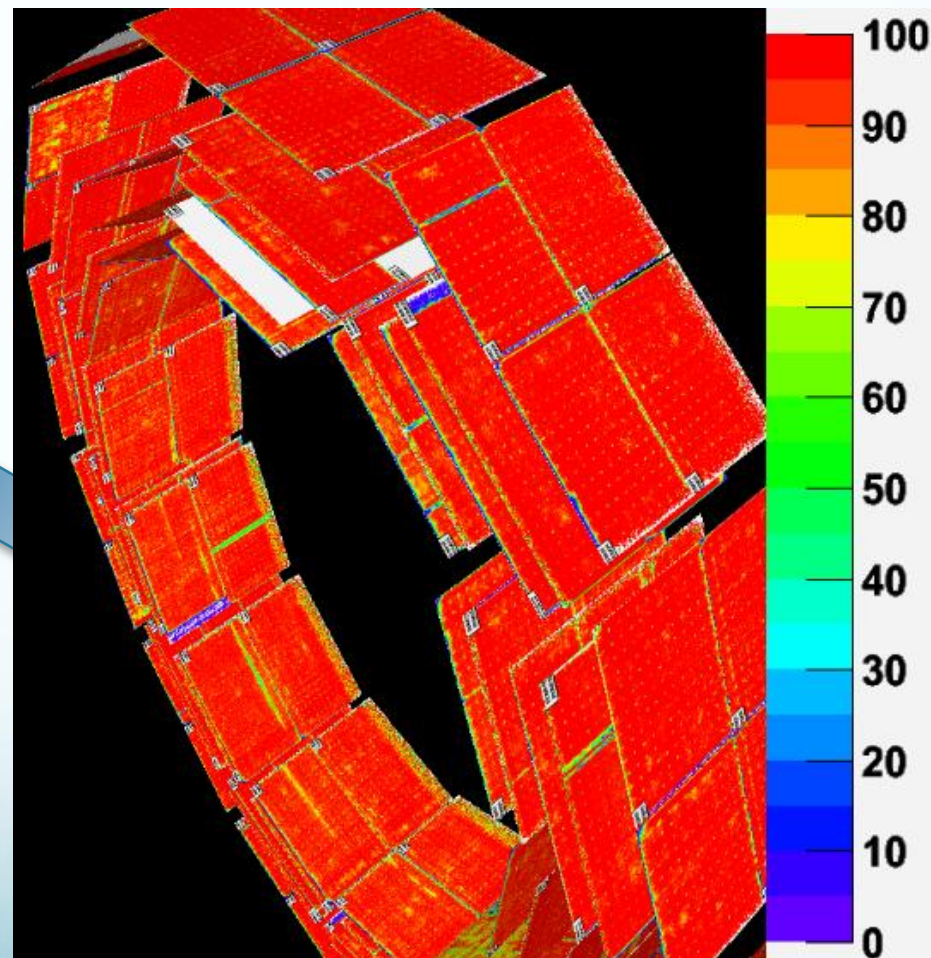
2D Efficiency map



CMS 2011 Preliminary $\sqrt{s} = 7$ TeV

Muon Radiography: the chamber efficiency can be studied in details, with a resolution of $\approx 1\text{cm}^2$. Spacers, border effects can be easily spotted. For few chambers, the stability in time of inefficient zones is under observation.
No degradation observed up to now.

3D efficiency view of one of the barrel wheels



CMS 2011 Preliminary $\sqrt{s} = 7$ TeV

DT Spatial resolution

Single hit resolution:

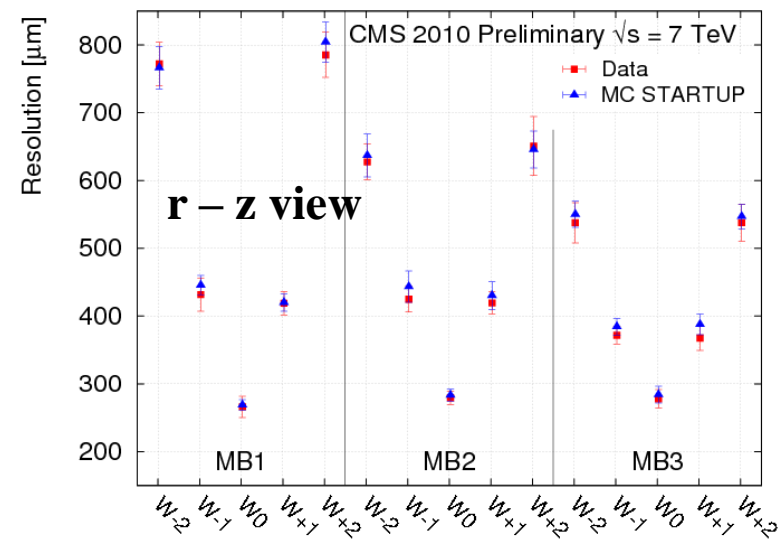
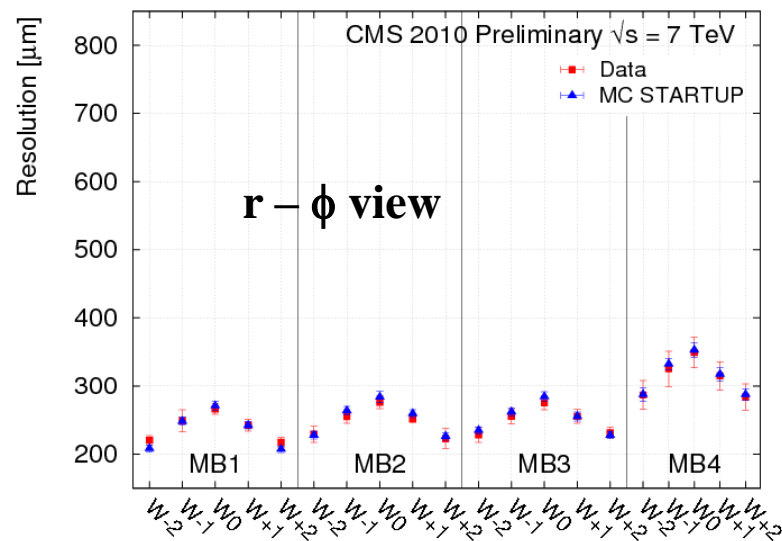
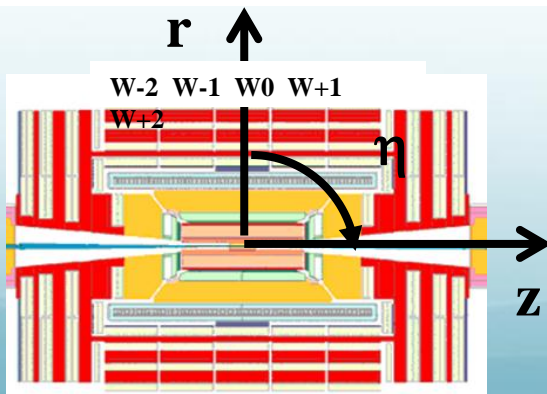
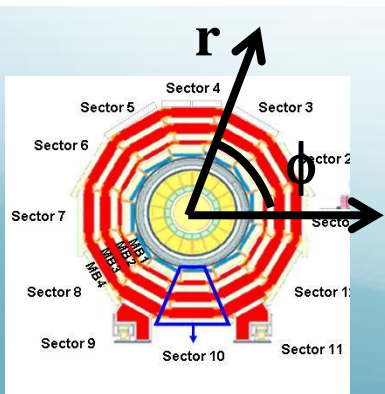
from the distribution of hit residuals with respect to the reconstructed segment.

$r - \phi$ view: $\approx 200-350 \mu\text{m}$

- get better at large η due to longer trajectory of particles at large angles of incidence
- worse in MB4 due to missing r-z super-layer

$r - z$ view $\approx 250-750 \mu\text{m}$

- get worse at large η due to larger angle of incidence on crossing particles (deviations from linearity)

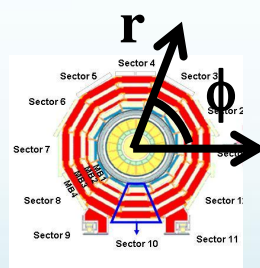
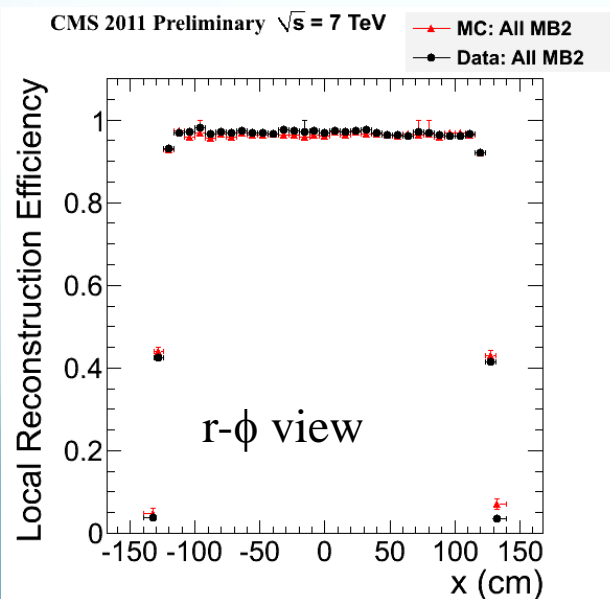


DT local reconstruction efficiency

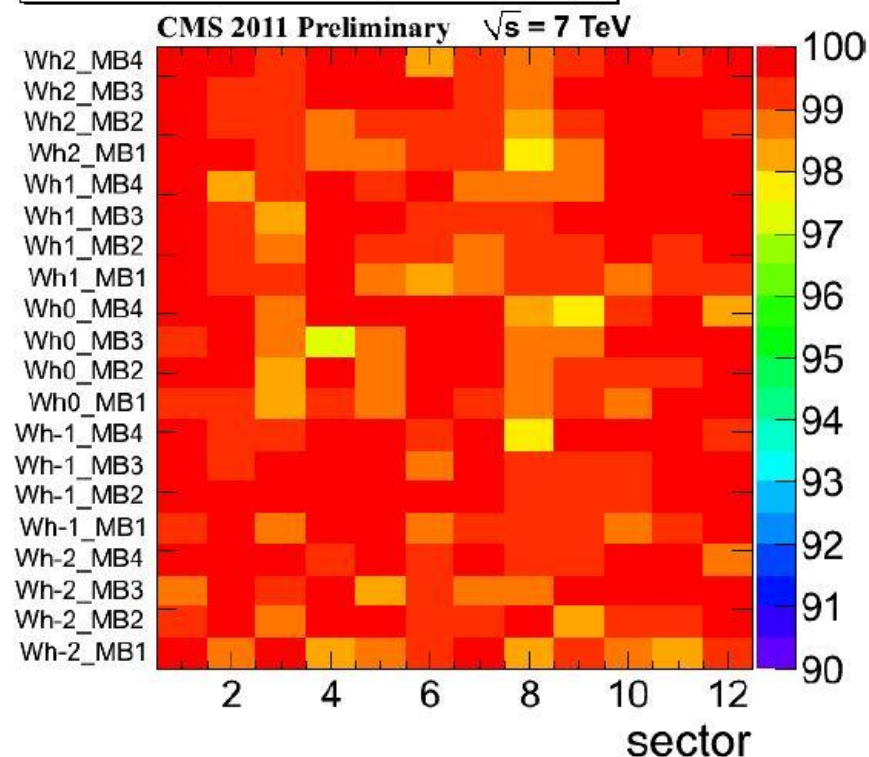
Local reconstruction efficiency:

Tag (a global muon) & **Probe** (a tracker track) method applied to di-muons from Z^0 decays.

Efficiency for all chambers > 97%



Local Reconstruction Efficiency



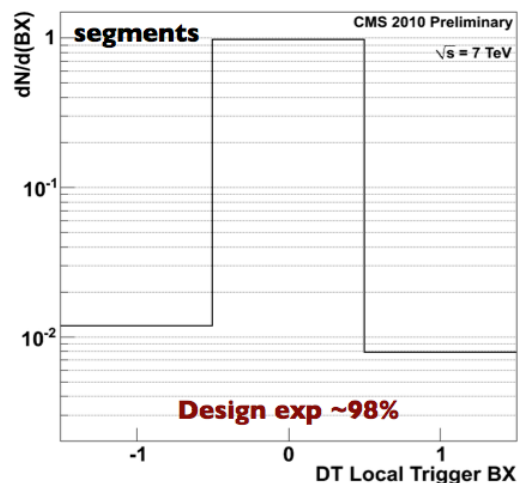
Segment reconstruction efficiency in all station 2 chambers in r - ϕ view.

Good agreement with Monte Carlo simulation.

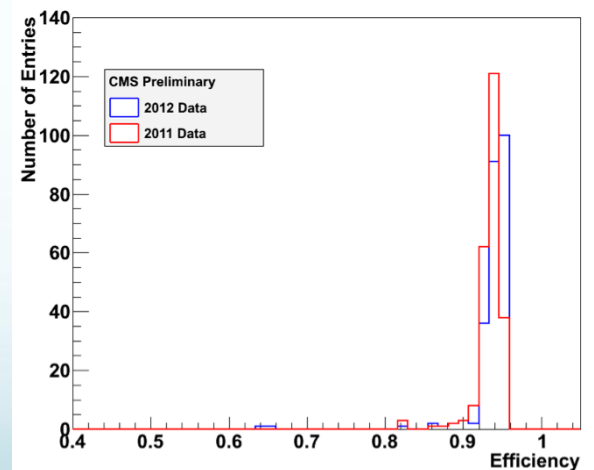
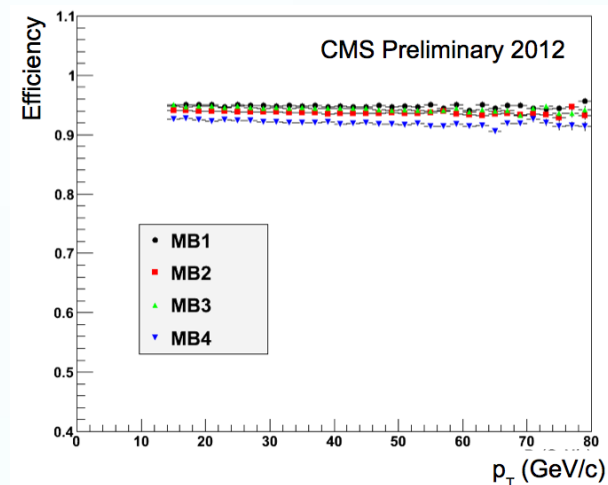
DT Local trigger performace

- **DT local trigger efficiency:** the presence of a trigger segment when there is a reconstructed track segment in the same chamber.
- the drop in MB4 is due to two known problematic chambers.

➤ System synchronization



Time distribution for DT: **98 % of highest quality DT trigger segments are in the correct BX**



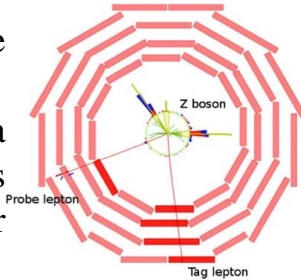
Average trigger efficiency: 93.5 % in 2011 and 93.7 % in 2012

RPC Trigger performance

- **RPC trigger efficiency: Tag & Probe method** on di-muons from J/Y and Z resonances.

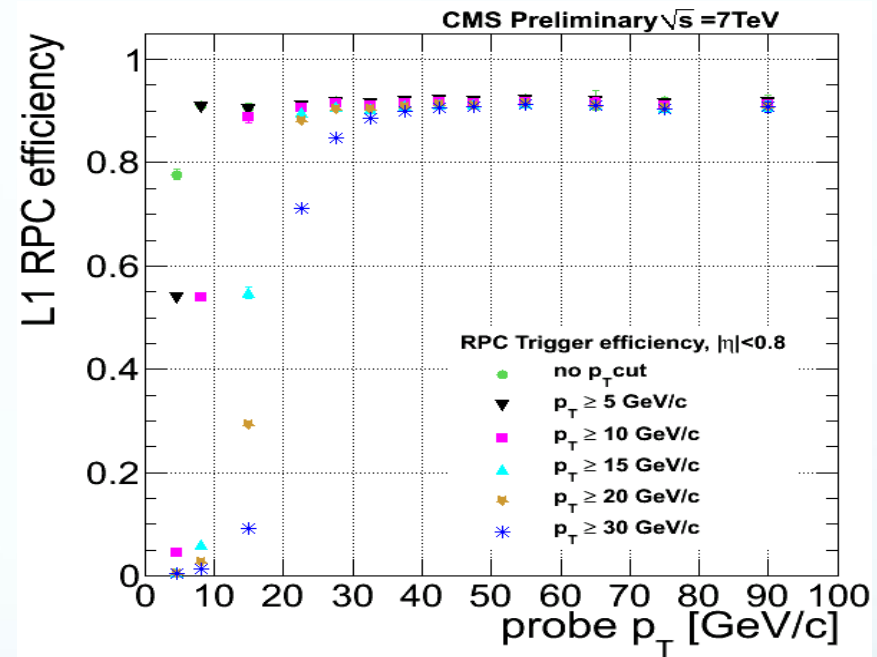
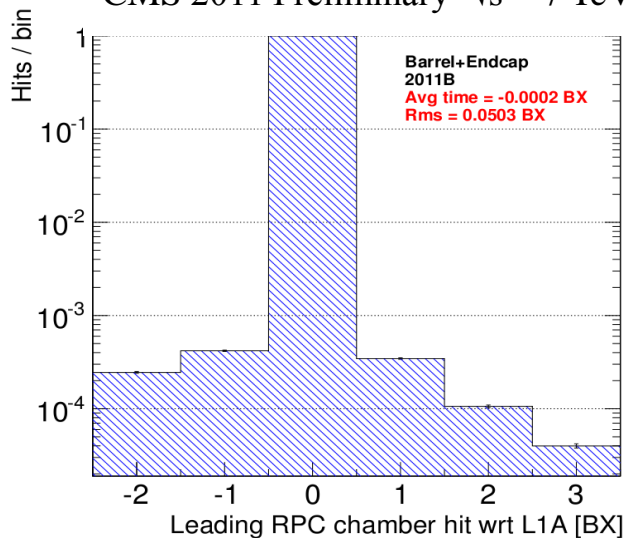
Tag is a global muon which triggers the event.

Probe is a tracker track (identified as a muon by the two-muon invariant-mass constraint). The efficiency is measured for the probe muon.



- **System synchronization**

CMS 2011 Preliminary $\sqrt{s} = 7$ TeV



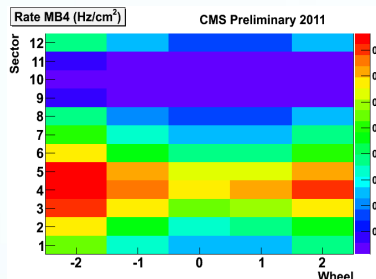
probe with $p_T > 20$ GeV/c from Z's
probe with $p_T < 20$ GeV/c from J/ ψ 's

L1 RPC efficiency above 90% in the barrel region.

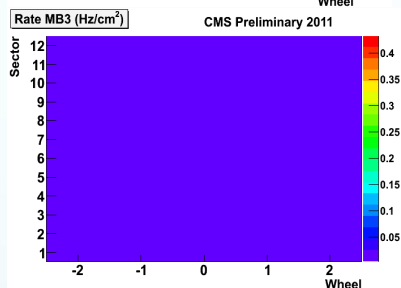
Time distribution for RPC: **99.89 % of RPC hits are in the correct BX.**

DT Background study

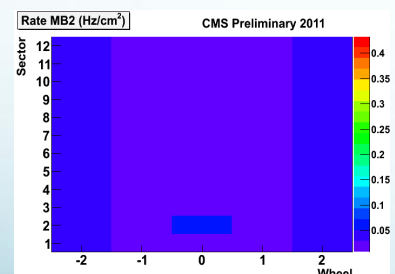
@ Inst. Luminosity $\sim 10^{33}$ Hz/cm²



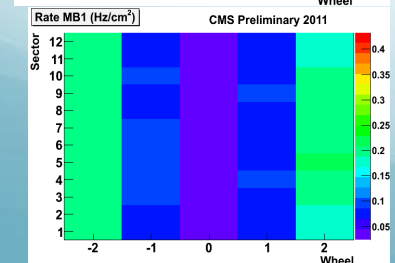
MB4



MB3



MB2

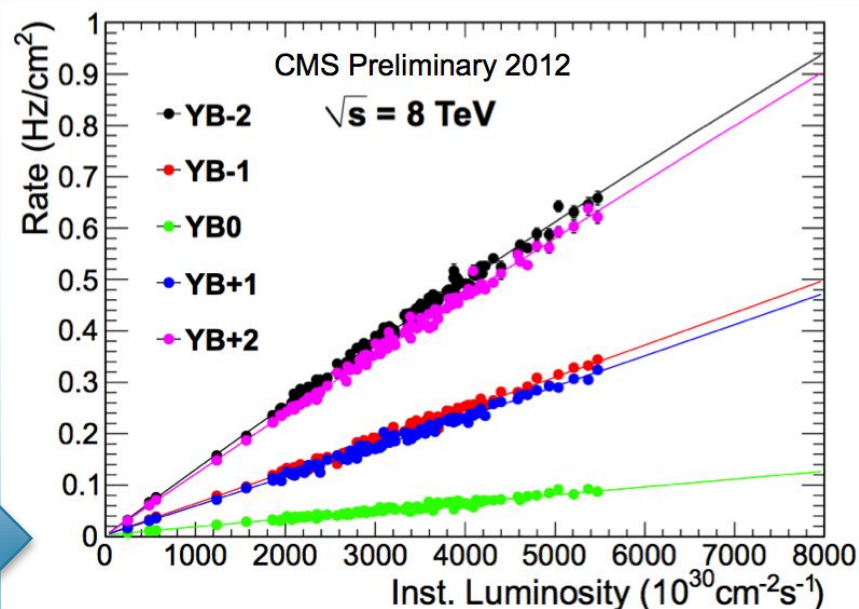


MB 1

Higher rate in:

- external wheels W+2 and W-2.
- outermost stations affected by slow neutron gas
- Innermost stations affected by Hcal particle leakage
- Top – bottom asymmetry due to wheels' supports and steel flooring

At luminosity of 10^{34} cm⁻²s⁻¹: **max rate < 5 Hz /cm²**



RPC Background study

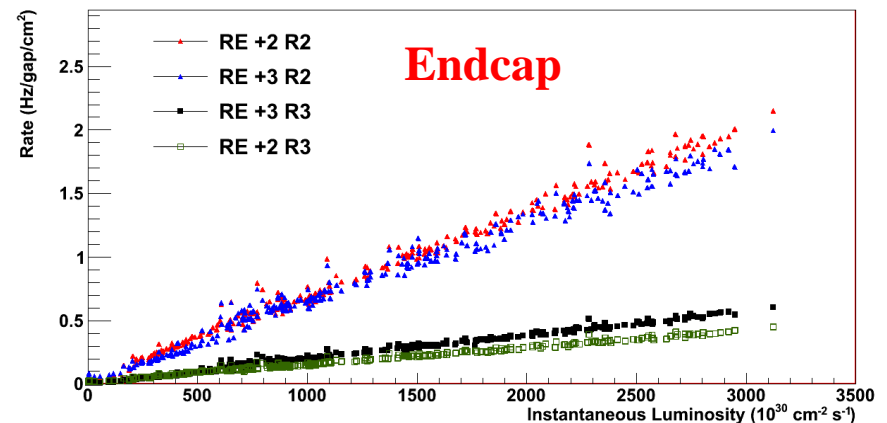
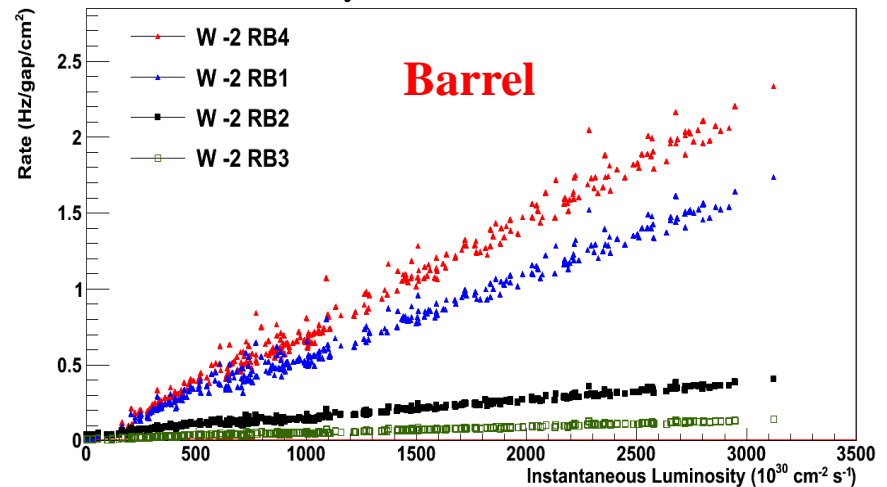
Background rate vs instantaneous luminosity

- **Barrel region:** same background pattern as measured by DT.
- **Endcap region:** higher rate in external disks and inner rings (RE+2 and RE+3 R2)

No significant issues with increases of luminosity up to $10^{34} \text{cm}^{-2} \text{s}^{-1}$:

- **max rate of 10 Hz/cm² (Barrel)**
20 Hz/cm² (Endcap)
- **Average rate $\approx 3 \text{ Hz/cm}^2$ (Barrel)**
 $\approx 6 \text{ Hz/cm}^2$ (Endcap)

CMS Preliminary 2011



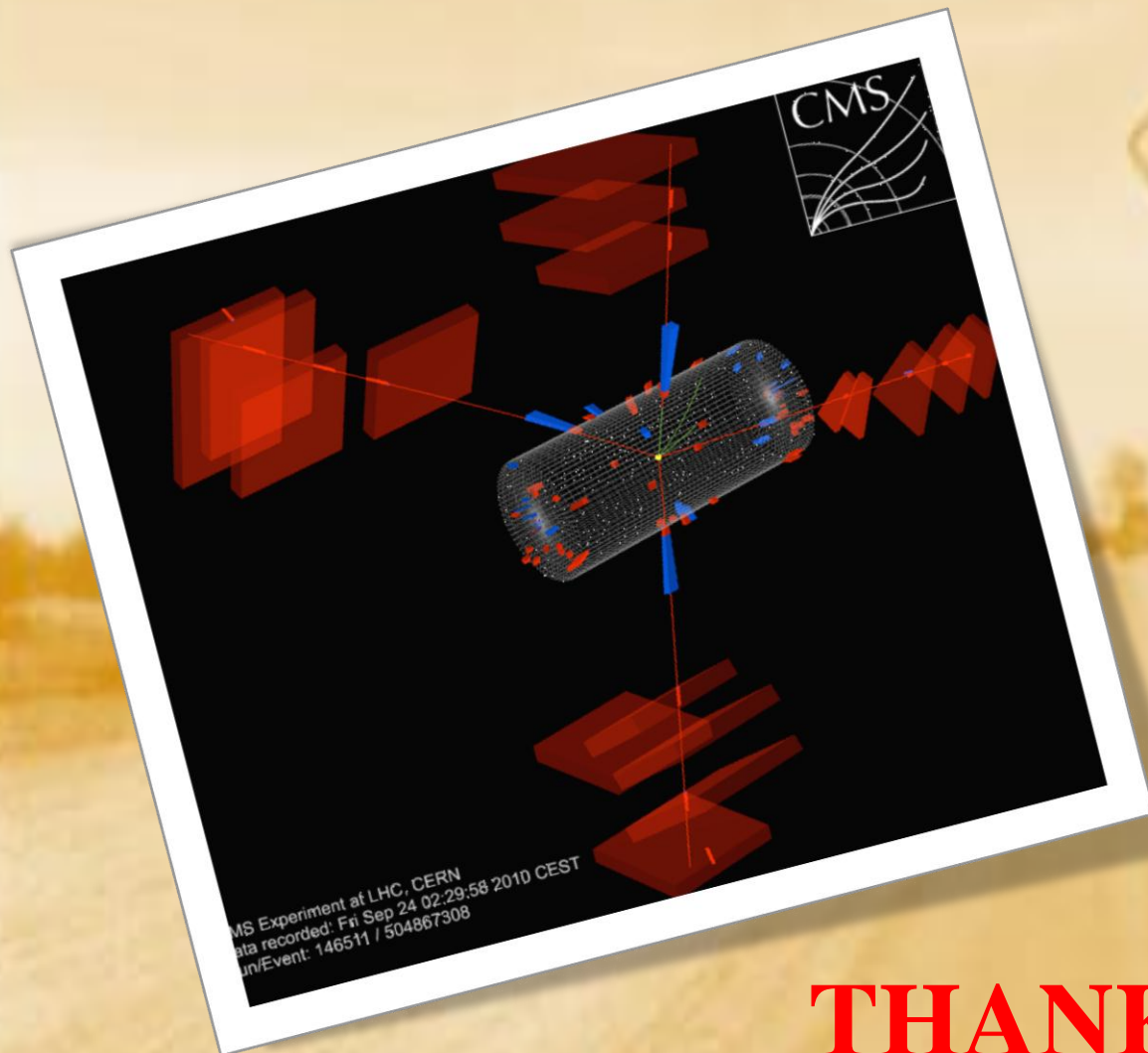
Conclusions

The CMS DT and RPC **systems are operating extremely well** delivering good triggers and data for physics:

- the contribution to the CMS downtime is very low: less than 1.5 %
- the fraction of active channels is very high and stable: more than 98%.

After 3 years of LHC running with increasing instantaneous luminosity and 6 years from the end of construction, the **detector performance** is within specifications both as triggering and as reconstruction system:

- The RPC performance is stable with no degradation observed. Efficiency more than 95 %.
- DT local reconstruction efficiency more than 97 %.
- Excellent synchronization and efficiency of the trigger system.
- Background measurements are within expectation. No significant issues for running at nominal luminosity.



THANKS!



Backup slides

The Large Hadron Collider

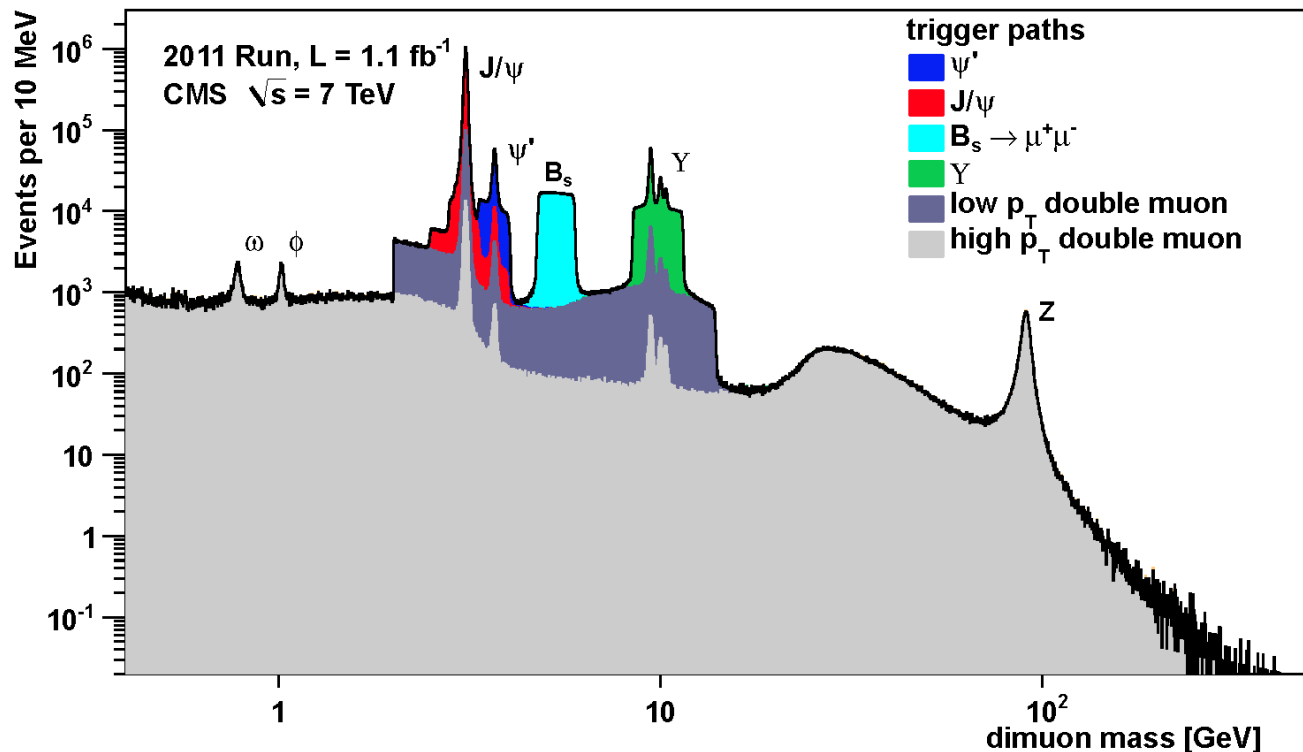


Large Hadron Collider is a proton-proton collider, with centre of mass collision energies of up to **14 TeV**. Installed 100 m underground in a tunnel 27 km long. Two high luminosity experiments, ATLAS and CMS, aiming at a peak luminosity of $10^{34} \text{ cm}^{-2}\text{s}^{-1}$.

	2010	2011	2012
Lumi Recorded	43.17 pb ⁻¹	5.561 fb ⁻¹	6.15 fb ⁻¹
Max lumi	2 x10 ³² Hz/cm ²	3.5x10 ³³ Hz/cm ²	6.64x10 ³³ Hz/cm ²
□s	7	7	8
Bunches spacing	75 ns	50 ns	50 ns

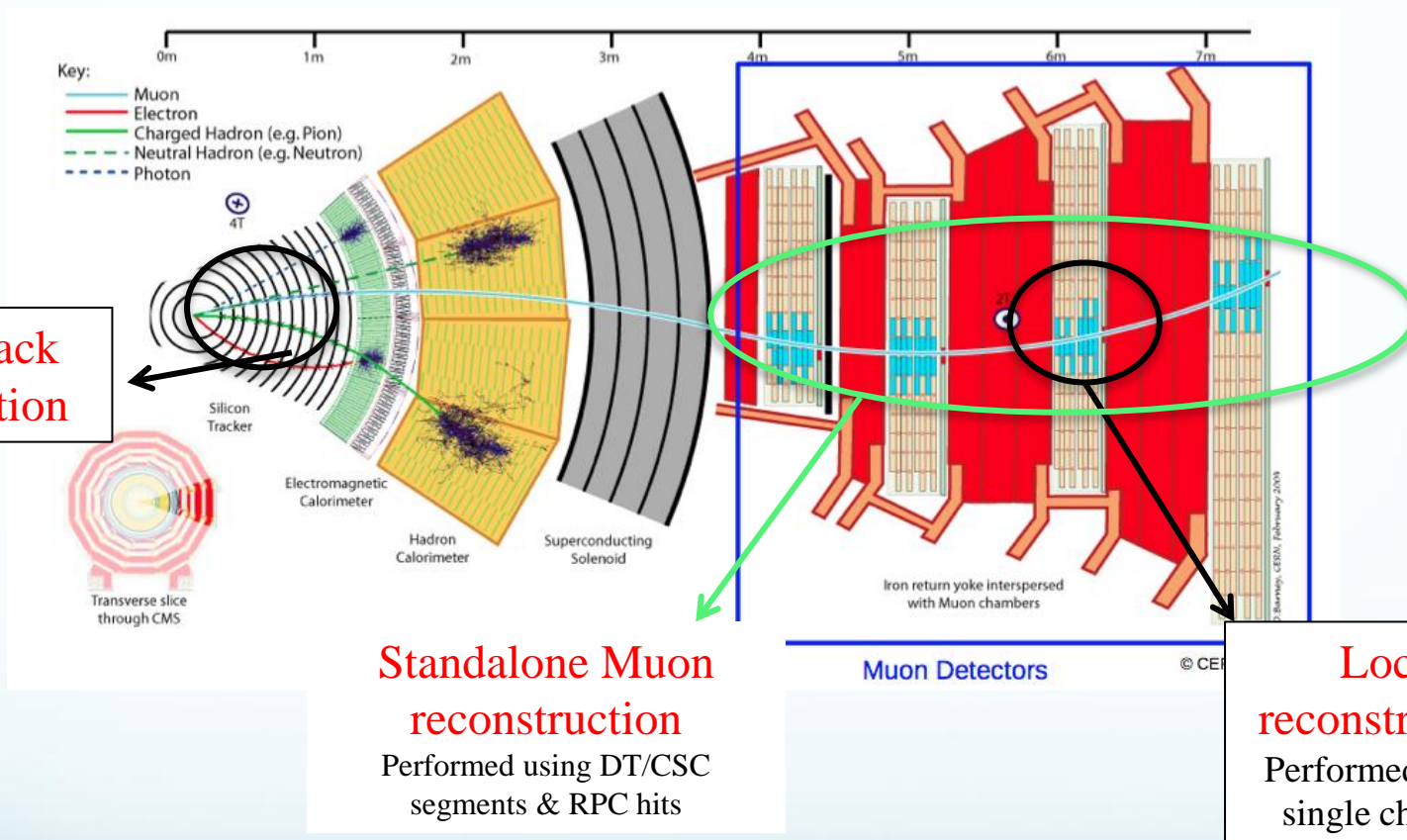
Triggering on di-muons in 2011

Impressive di- μ spectrum!!!



Dimuon mass distribution obtained from overlapping several trigger paths.
Dimuon triggers fundamental for searches but used also for calibrations

Muon Reconstruction



Global muon reconstruction (out side –in): a standalone muon is propagated to match a tracker track. If matching is positive a global fitting is performed.

Tracker Muon (inside – outside): a tracker track is propagated to muon system and qualified as muon if matching with standalone or one segment.

RPC



Barrel and Endcap chambers have different geometries and have been built in different sites with different construction techniques.

- **Gaps:** in Italy for the Barrel and Korea for Endcap
- **Chambers:** Bulgaria and Italy for Barrel and China, Pakistan and Cern for endcap.

RPC in the muon reconstruction

G. Pugliese

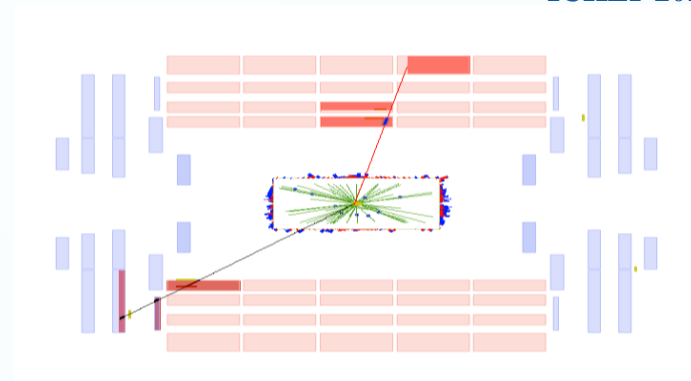
ICHEP 2012

Example of a track (in red, 1 DT segment + 2 RPC hits) that will fail in reconstruction if the RPC hits are removed in the track fitting

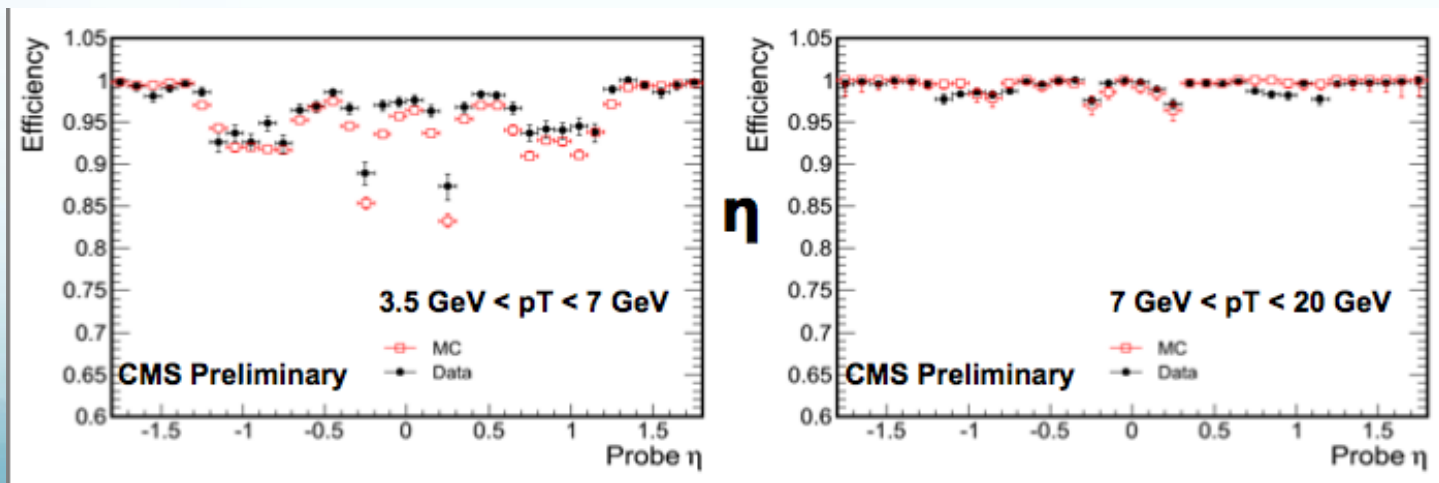
tag-and-probe method using J/Ψ resonance

Probes: Muons reconstructed with RPC hits

Passing Probes: Muons reconstructed without RPC hits



$$\text{efficiency} = \frac{\text{Passing probes}}{\text{Probes}}$$



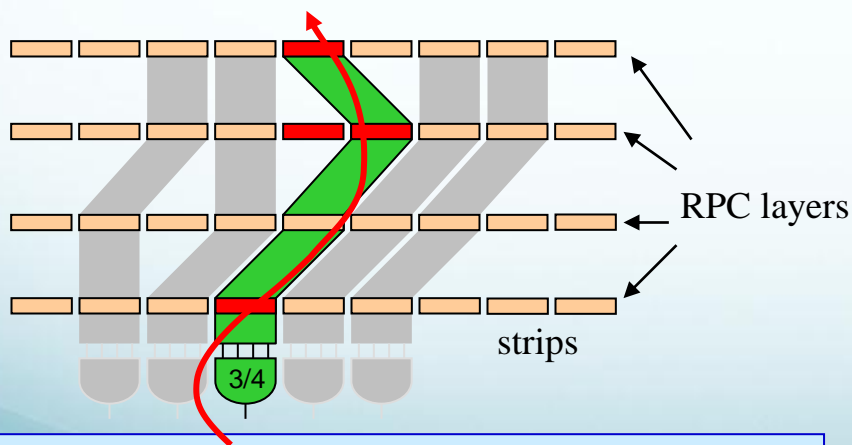
RPC hit contribution is more evident for $pT < 7$ GeV and in the crack regions between adjacent wheels

RPC trigger algorithm: Pattern Comparator (PAC)

The RPC hits are compared with the **predefined set of patterns**.

Each pattern has assigned a **transverse momentum (p_T)** and **sign** (depending on the track banding by the magnetic field).

Muon candidate is recognized if RPC hits fit to the pattern and are in the same 25 ns clock period (BX)



A pattern is a set of AND gates connected to selected strips

A muon candidate is produced even though not all layers have hits.

The minimum required number of fired layers is 3 (out of 3, 4, 5 or 6 layers available, depending on a detector region).

In this way the trigger efficiency does not suffer from the limited geometrical acceptance and inefficiency of the chambers.

The **number of fired planes** defines the **candidate quality**.

The quality is used for the candidates sorting and “ghost busting” (cancellation of duplicated candidates).

RPC Trigger

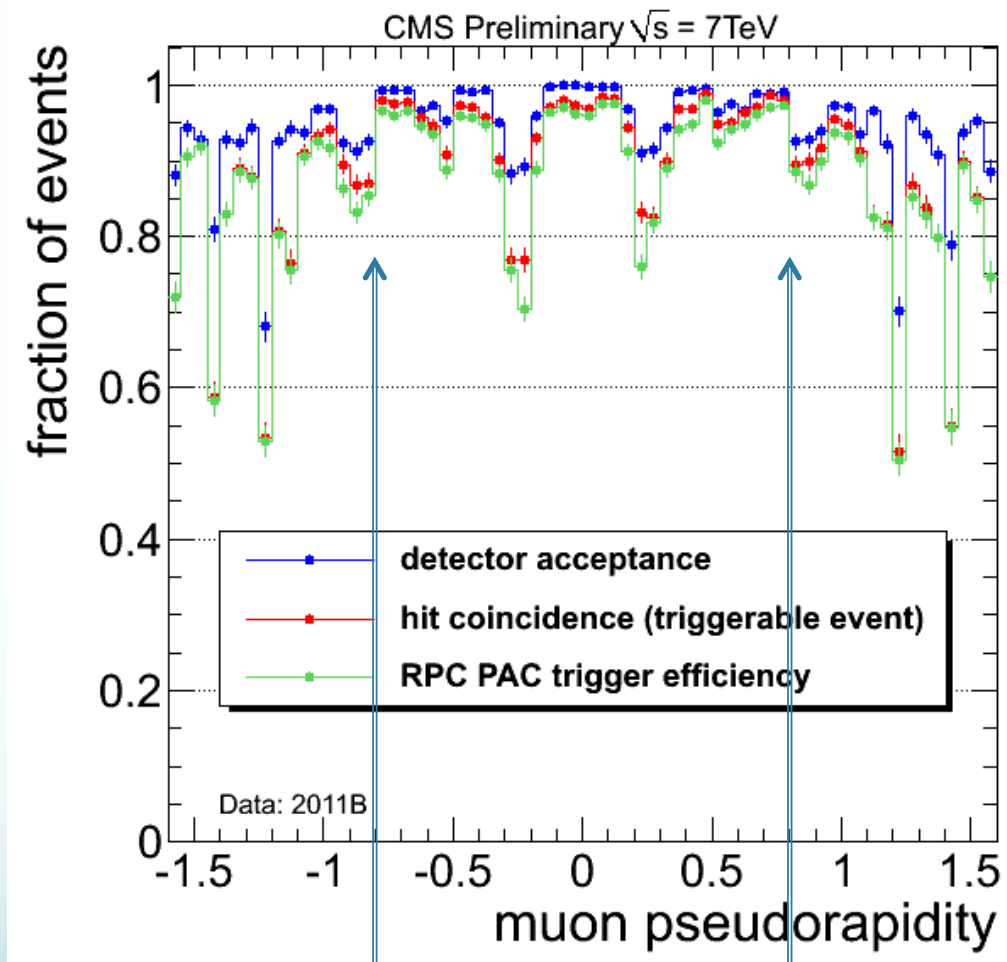
The efficiency of RPC PAC trigger for identifying muons is a convolution of:

- $\epsilon_{\text{acceptance}}$ – geometrical acceptance of the RPC detector (fraction of muons crossing at least 3 chambers),
- $\epsilon_{\text{chambers}}$ – chambers intrinsic efficiency,
- $\epsilon_{\text{patterns}}$ – patterns efficiency i.e. probability that the chamber hits of a **“triggerable” muon** fit to any pattern;

“triggerable” muon – hits in at least 3 RPC layers inside the eta-phi cone covered by one PAC unit and in the same BX

$$\epsilon_{\text{triggerable muon}} = \epsilon_{\text{acceptance}} \otimes \epsilon_{\text{chambers}}$$

Good quality offline muons compatible with vertex, with $p_T > 10 \text{ GeV}/c$, matching the RPC candidate. Minium-bias dataset.



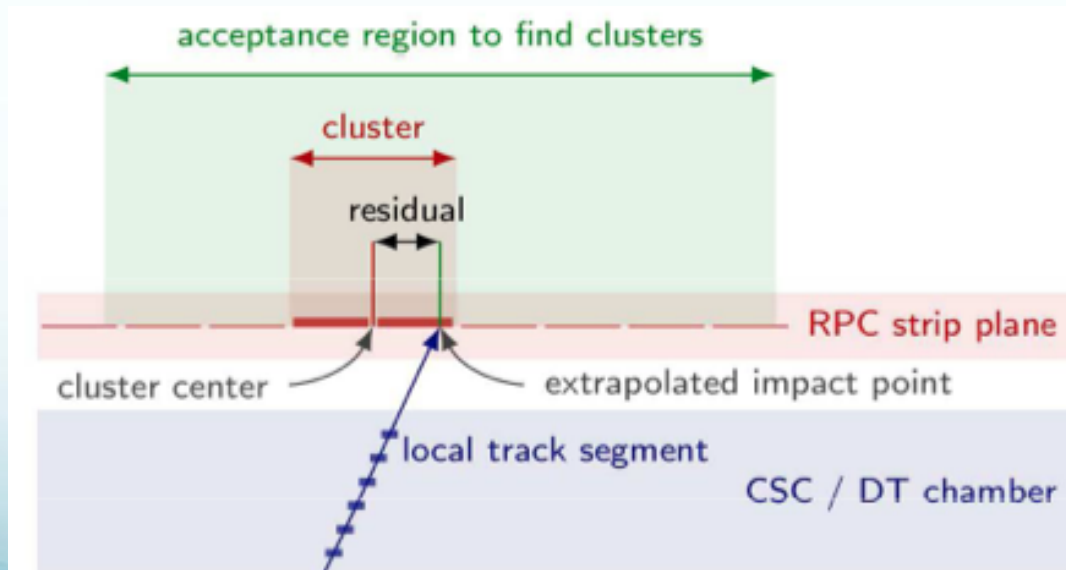
Endcap

Barrel

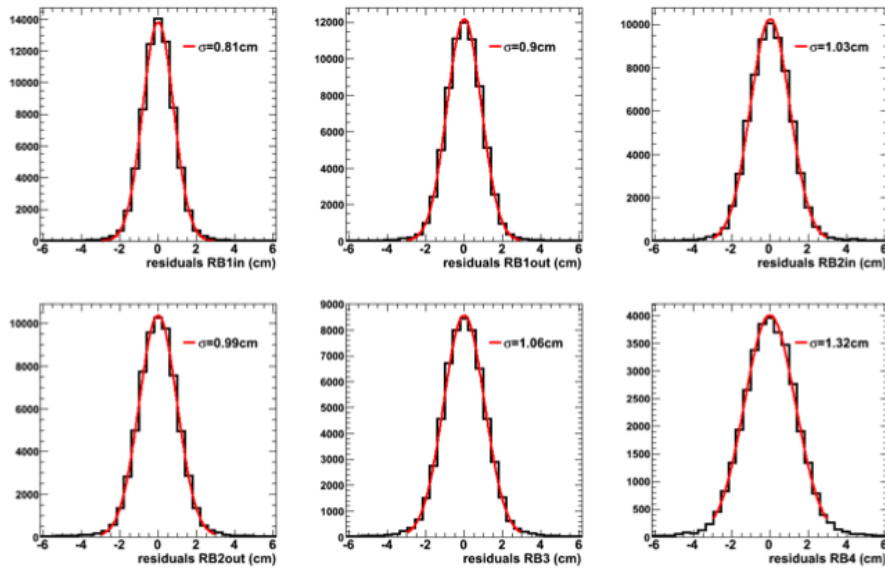
Endcap

Method to study the RPC performance

Segment extrapolation method: a DT/CSC segment of high quality, associated to a stand-alone muon track, is extrapolated to RPC strip plane. For each extrapolated impact point, the RPC efficiency is computed looking at RPC Hits in a range of ± 2 strips from the extrapolated point



RPC spatial resolution

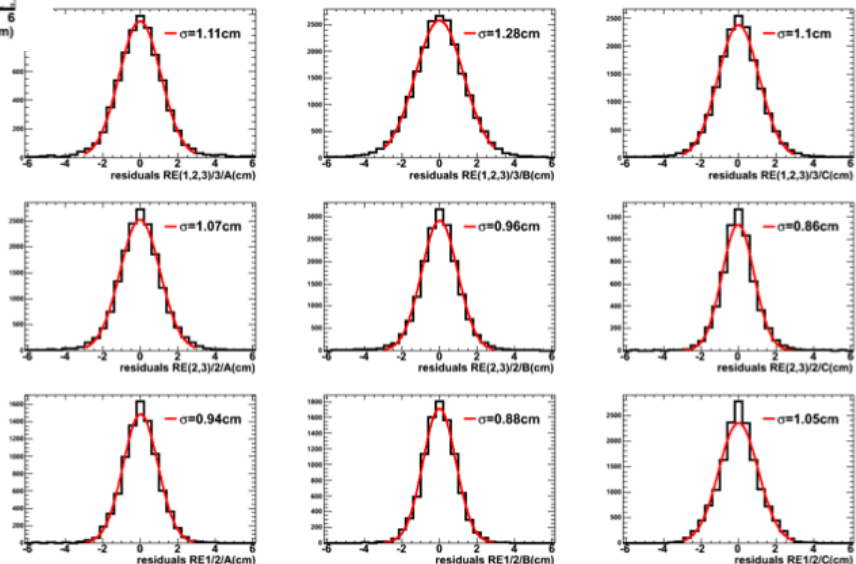


Barrel: from $\sigma = 0.81$ cm in the inner, to $\sigma = 1.32$ cm in the outer station.

Strip widths range from 2.28 cm to 4.10 cm

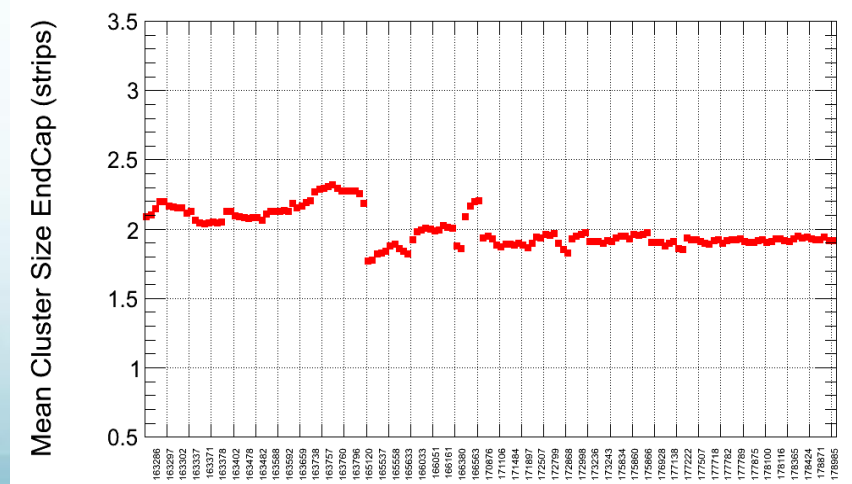
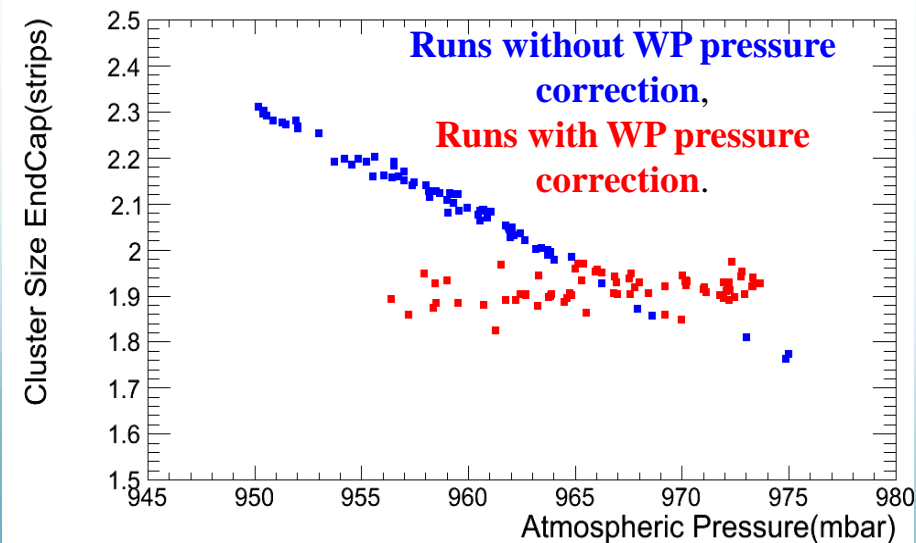
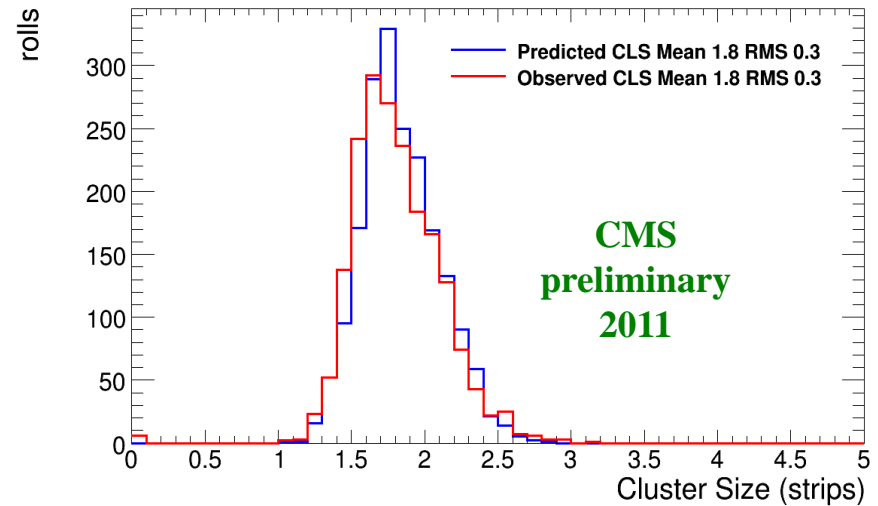
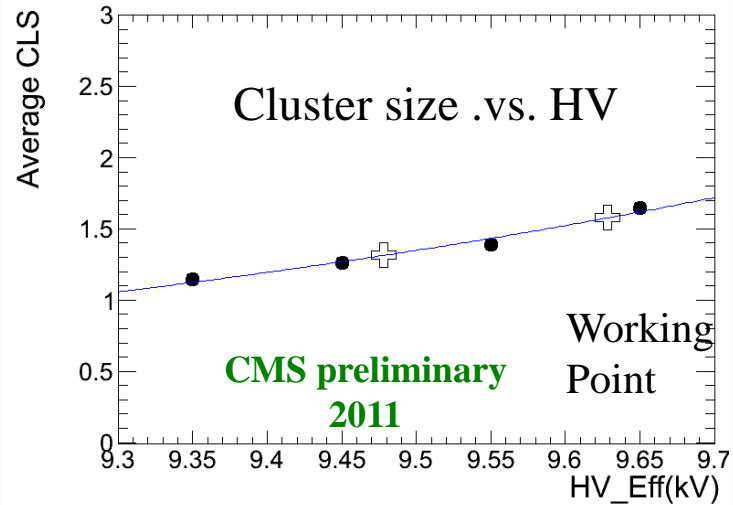
Endcap: $\sigma = 0.86$ cm in the inner, to $\sigma = 1.28$ cm in the outer ring.

Average strip widths range from 1.95 cm to 3.63 cm

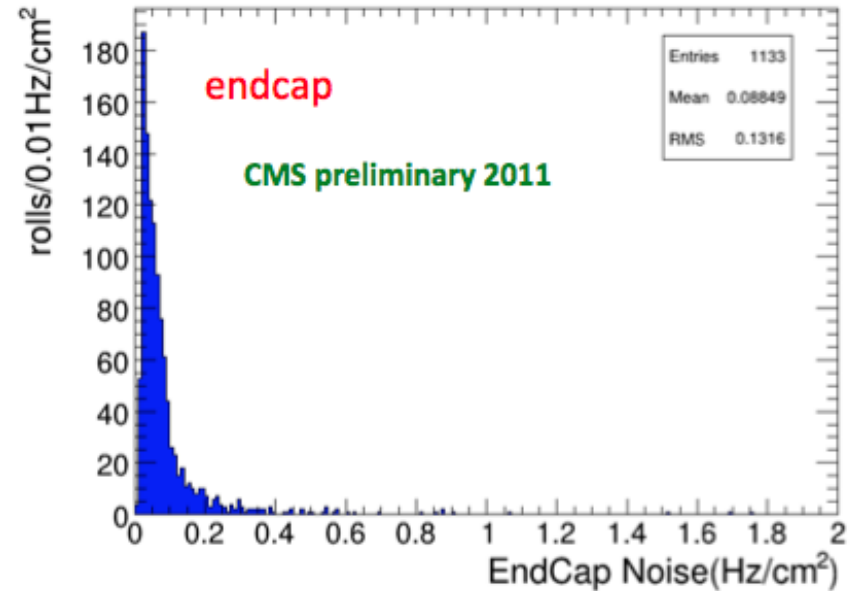
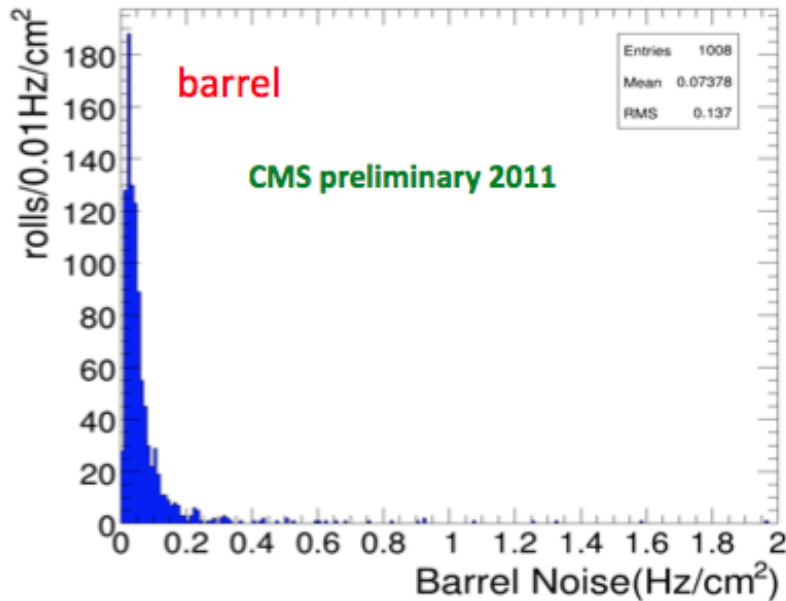


Chamber performance: cluster size

G. Pugliese



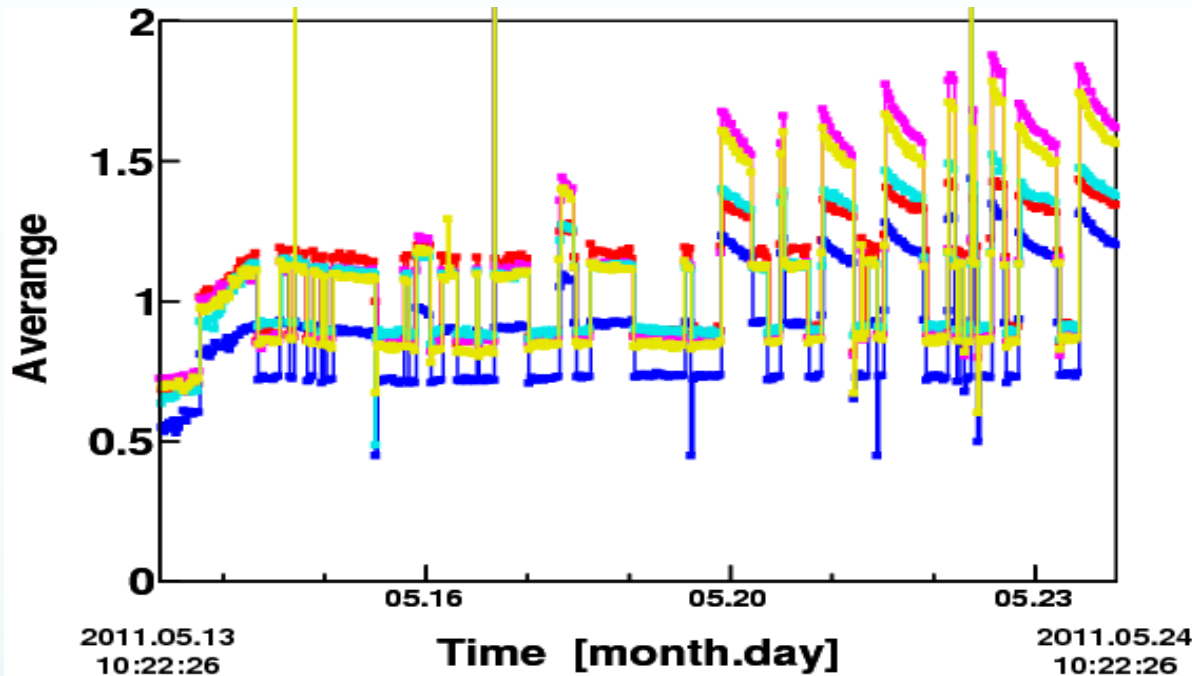
RPC noise



Noise distribution for all barrel and endcap chambers at WP operation. The average value is $\sim 0.08 \text{ Hz/cm}^2$

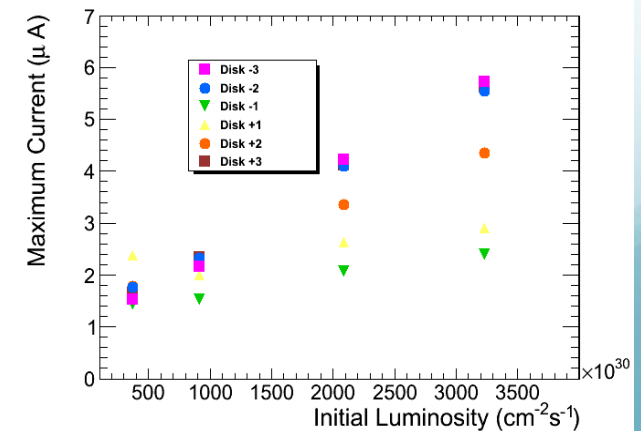
RPC Monitoring of the current

G. Pugliese



Current is correlated to the beam intensity

Current without beam is stable in time



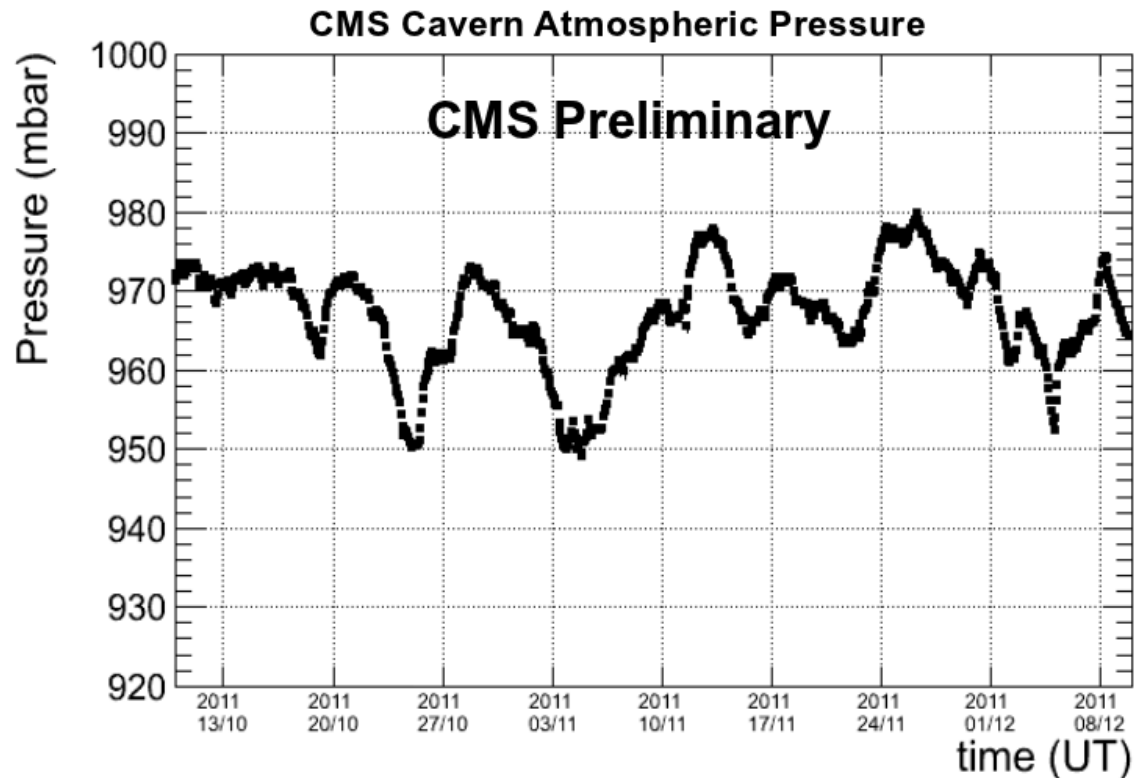
Atmospheric Pressure monitoring

HV working point is calculated taking into account the pressure variations

$$HV_{\text{effective}} = HV \cdot P_0/P \cdot T/T_0$$

$P_0 = 965 \text{ mbar}$, $T_0 = 293 \text{ K}$

$\sim 1\% \text{ P variation} = \sim 100 \text{ V difference}$

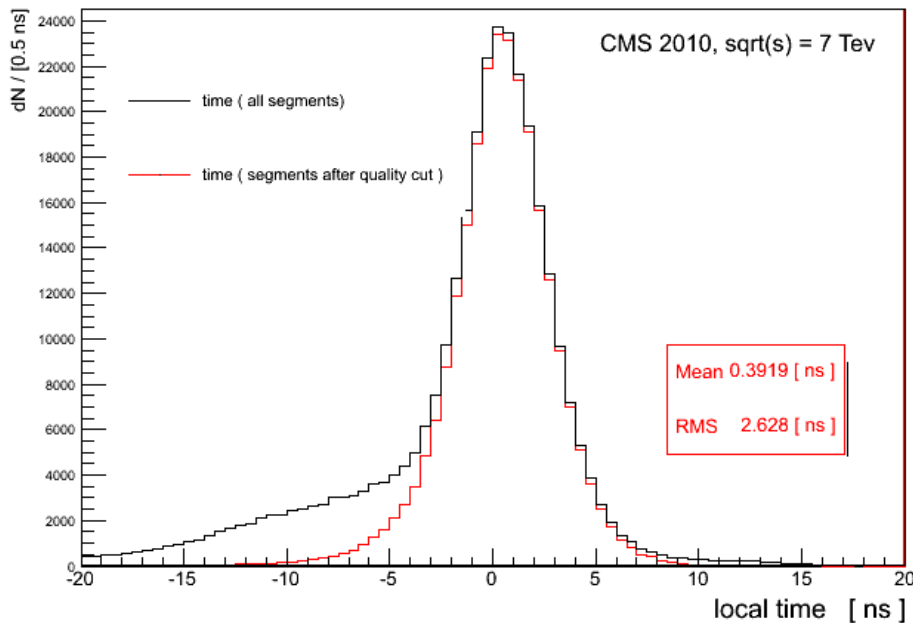


DT time resolution

In addition to the measurement of the track position and direction, DT provides a measurement of the arrival time of the track to the chamber.

The arrival time of a track in each DT chamber is reconstructed allowing a **common displacement of the hits from the wire position** to be a free parameter in the segment fit.

Assuming V_{drift} constant \Rightarrow common displacement \equiv shift in the time of the track



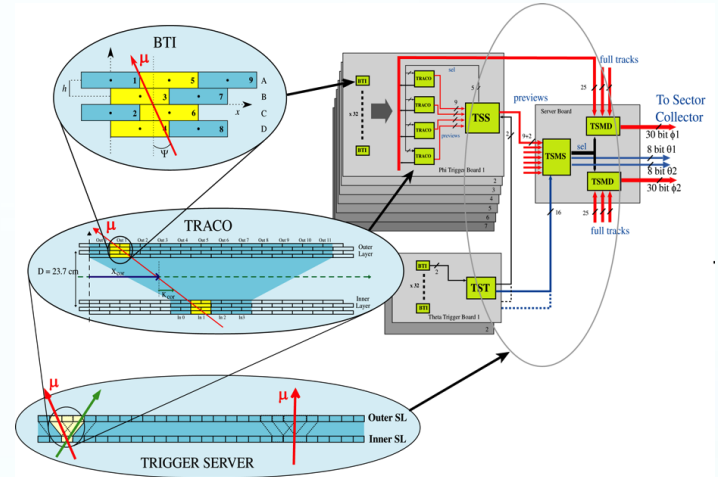
The black distribution shows a clear tail due to the presence of δ -rays.

The red distribution shows the local time for segments passing a χ^2 quality cut.

Measured local time distribution for all chambers for all stations.

DT plan for LS1

The DT Local Trigger is implemented using dedicated electronics located both on the chambers (**minicrates**) and on the balconies surrounding the detector, the **Sector Collector (SC)**.



Replacement of theta TRB (Trigger boards): Minicrates contain TDCs and BTI (ASIC wire bond) which are obsolete, no more ASICs can be produced, and sensitive to thermal stress during switch on/off. Current stock of spares is a potential issue. **Plan:** replace theta TRB (in MB1 and 2 in W+2/-2) with the new boards based on FPGA. Cannibalize BTIM from replaced boards to enlarge number of TRB ϕ and θ spares.

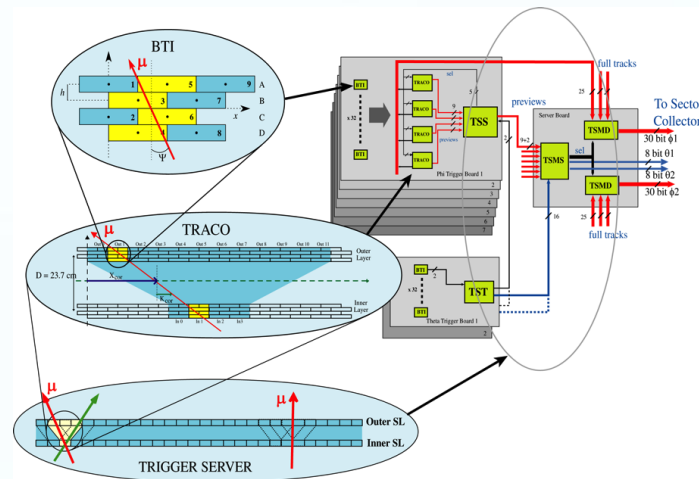
Relocation of Sector Collector from the cavern (UXC) to the counting room (USC): the flow of Minicrate data goes through the Sector Collectors (one per wheel) in the detector towers. This can constitute a potential single failure points, given the limited access to UXC. All Minicrates will be connected to USC with optical fibers.

DT Trigger

G. Pugliese

1. **The DT Local Trigger** is implemented using dedicated electronics located both on the chambers (**minicrates**) and on the balconies surrounding the detector, the **Sector Collector (SC)**.

BTIs: the signals coming from single wires are initially processed by Bunch and Track identifiers (**BTIs**) that operate rough track fitting within a single SL and perform BX assignment.



TRACOs: the Track Correlators (TRACOs) is devoted to match the information coming from the two ϕ - SLs and improve the parameter measurements.

TS: the Trigger Server (TS) performs a quality based selection on the segments coming from different TRACOs.

SC: information from chambers of a single sector is forwarded, on the balconies surrounding the detector, to the Sector Collector (SC) that has to further refine the sorting, perform synchronization on data coming with different latencies, and send the signal to the DT Regional Trigger.

2. **The DT Regional Trigger** performs correlation between the track segment received by the SC boards in order to build full muon tracks. Best track candidates are selected by the Muon Sorter and (up to) four candidates per BX are send to the Global Muon Trigger.